
Article:
Alkahtani, Mohammed, Hu, Yihua, Alghaseb, Mohammed A. et al. (4 more authors) (2020) Investigating fourteen countries to maximum the economy benefit by using offline reconfiguration for medium scale pv array arrangements. Energies. 59. ISSN 1996-1073

https://doi.org/10.3390/en14010059

---

energies

MDPI

Article

Investigating Fourteen Countries to Maximum the Economy Benefit by Using Offline Reconfiguration for Medium Scale PV Array Arrangements

Mohammed Alkahtani [1], Yihua Hu [2], Mohammed A Alghaseb [3], Khaled Elkhayat [3], Colin Sokol Kuka [2,*], Mohamed H Abdelhafez [3,4] and Abdelhakim Mesloub [3]

1 Electrical Engineering and Electronics Department, University of Liverpool, Liverpool L69 3GJ, UK; m.alkahtani@liverpool.ac.uk
2 Electronic Engineering Department, University of York, York YO10 5DD, UK; yihua.hu@york.ac.uk
3 College of Engineering, University of Hail, P.O. Box 2240, Hail, Saudi Arabia; ma.alghaseb@uoh.edu.sa (M.A.A.); k.elkhayat@uoh.edu.sa (K.E.); mo.abdelhafez@uoh.edu.sa (M.H.A.); a.maslub@uoh.edu.sa (A.M.)
4 Architecture Engineering Department, Aswan University, 81528 Aswan, Egypt
* Correspondence: sk1759@york.ac.uk; Tel.: +44-07405-33-3261

Abstract: Over the past few years, electricity demand has been on the rise. This has resulted in renewable energy resources being used rapidly, considering the shortage as well as the environmental impacts of fossil fuel. A renewable energy source that has become increasingly popular is photovoltaic (PV) energy as it is environmentally friendly. Installing PV modules, however, has to ensure harsh environments including temperature, dust, birds drop, hotspot, and storm. Thus, the phenomena of the non-uniform aging of PV modules has become unavoidable, negatively affecting the performance of PV plants, particularly during the middle and latter duration of their service life. The idea here is to decrease the capital of maintenance and operation costs involved in medium- and large-scale PV power plants and improving the power efficiency. Hence, the present paper generated an offline PV module reconfiguration strategy considering the non-uniform aging PV array to ensure that this effect is mitigated and does not need extra sensors. To enhance the economic benefit, the offline reconfiguration takes into account labor cost and electricity price. This paper proposes a gene evolution algorithm (GEA) for determining the highest economic benefit. The proposed algorithm was verified using MATLAB software-based modeling and simulations to investigate fourteen countries to maximize the economic benefit that employed a representative 18-kW and 43-kW output and the power of 10 × 10 PV arrays in connection as a testing benchmark and considered the electricity price and workforce cost. According to the results, enhanced power output can be generated from a non-uniformly aged PV array of any size, and offers the minimum swapping/replacing times to maximize the output power and improve the electric revenue by reducing the maintenance costs.

Keywords: solar photovoltaic; rearrangement; non-uniform aging; reconfiguration; gene evaluation algorithm; maintenance cost; electric revenue

Citation: Alkahtani, M.; Hu, Y.; Alghaseb, M.A; Elkhayat, K.; Kuka, C.S.; Abdelhafez, M.H; Mesloub, A. Investigating Fourteen Countries to Maximum the Economy Benefit by Using Offline Reconfiguration for Medium Scale PV Array Arrangements. *Energies* **2021**, *14*, 59. https://dx.doi.org/10.3390/en14010059

Received: 5 December 2020
Accepted: 22 December 2020
Published: 24 December 2020

1. Introduction

In the last 10 years, the increased greenhouse gas emissions resulting from fossil fuels being excessively used and the requirement of saving these resources has led to the necessity of using renewable energy, particularly solar energy using photovoltaic (PV) plants.

PV modules tend to be located in an exacting outdoor environment and are thus damaged by various factors such as storms, wind, bird droppings, and hail, which leads to the modules becoming non-uniformly aged, thus adversely impacting their efficiency as well as the array's overall efficiency [1]. However, the differences in the cell characteristics

of a module involve other factors concerning the modules' non-uniform aging. An aged PV array's performance can be easily and rapidly improved by replacing the aged modules with new ones. However, not only can this be economically costly for the power plant owner, but the discrepancy in the specifications of other modules that were previously healthy with replaced modules as well as the bucket effect phenomenon may hinder the extraction of the best power of the array [2,3].

An aged PV cell's power decreases below its rated power. This reduction in the cell's short circuit current is significantly more sensitive compared to a reduction in the cell's open-circuit voltage, and thus, an aged cell's short-circuit current is used to indicate the cell's health [4–6]. Considering the fact that a PV module ages unevenly, every PV module is regarded as a series of three connected submodules that have varied aging conditions [7,8].

To enhance a PV array's output power, typically in the mismatch condition, different online as well as offline methods that have definite or heuristic algorithms have been presented. In [9–11], online rearrangement methods were implemented for enhancing the mismatched PV array's efficiency. However, these methods have the drawbacks of involving complicated computations and needing expensive switches and relays. In [2], a series-parallel array, despite the modules' non-uniform aging, involved every module's health status being indicated using a single short-circuit current, which led to considerable reduction in the calculations. Hence, a definitive offline rearrangement algorithm was introduced for improving the efficiency of the PV array.

Moreover, the advancement in materials technologies has ensured the economic production of monocrystalline silicon as well as multi-crystalline silicon in substantial quantities. On the other hand, the efficiency of their energy conversion from solar to electricity remains low. The typical efficiency of monocrystalline silicon solar cells is approximately 20% and that of multi-crystalline silicon solar cells is 18% [12,13]. Regarding power electronics, implementing high-performance switching devices such as super junction MOSFETs and silicon carbon and innovative converter topologies such as multilevel DC–DC as well as resonant DC–AC converters can enhance the efficiency of energy conversion [14,15]. This aspect of energy conversion efficiency can increase to 95% [14]. It should be noted, however, that these figures indicate the PV cells' nominal and healthy operation, but they can undergo different faults and aging conditions that can reduce the PV cells' lifetime as well as their operational efficiency [16]. In terms of such faulty or aged PV systems, energy efficiency can be easily improved by replacing aged PV modules with new ones. This, however, is not economically viable for most owners of PV system. Thus, the present paper proposes a reconfiguration strategy concerning aged PV systems to improve the maximum power generation by rearranging the positions of the PV modules while decreasing labor cost. This proposed reconfiguration strategy is based on the bucket effect concerning the maximum short-circuit current of PV strings and minimizing the swap times, for which it is important to introduce a PV system's basic structure and working principles.

A PV system involves three levels of components: the PV cell unit, PV module, and PV array (Figure 1). To limit the PV module hotspots, a bypass diode is connected parallel with the PV cells. This structure is called a cell unit (which includes m PV cells). In this PV system, assume that n cell-units are linked in a series forming a PV module to increase the output voltage and that s PV modules are linked in a series for developing a PV string. Different PV strings are connected using diodes and in parallel to form a PV array. It is possible for the diodes to stop the current flow between the strings, but this can be harmful.

In order to achieve quick calculation with low computing resources, this paper proposed a genetic-algorithm-supported reconfiguration for medium and large PV arrays exhibiting non-uniform aging. Therefore, the strategy offers the minimum swapping/replacing times to maximize the output power and to improve the electric revenue by reducing the maintenance cost. However, solar power plants can achieve better financial increments within a decade. The rest of this paper is organized as follows. Section 2 presents the electrical characteristics of PVs. In Section 3, we discuss the offline reconfiguration

strategy. Section 4 describes the photovoltaic array reconfiguration optimization scheme. Section 5 shows the cases of studies and simulation results, Section 6 is the analysis of outcomes, and our conclusions are presented in Section 7.

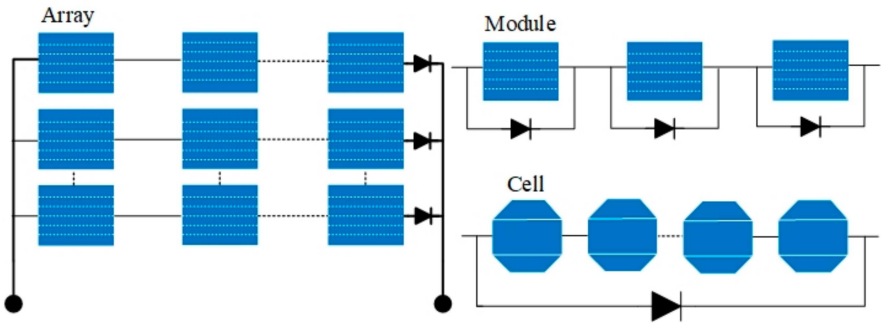

Figure 1. Componential structure of the photovoltaic (PV) array.

2. Electrical Characteristics of Photovoltaics (PVs)

Although the PV module has solar cells that directly convert solar irradiance into DC electricity by the photovoltaic effect, the PV array consists of a number of series-connected (NS) and parallels connected modules (NP) [17], as shown in (Figure 2).

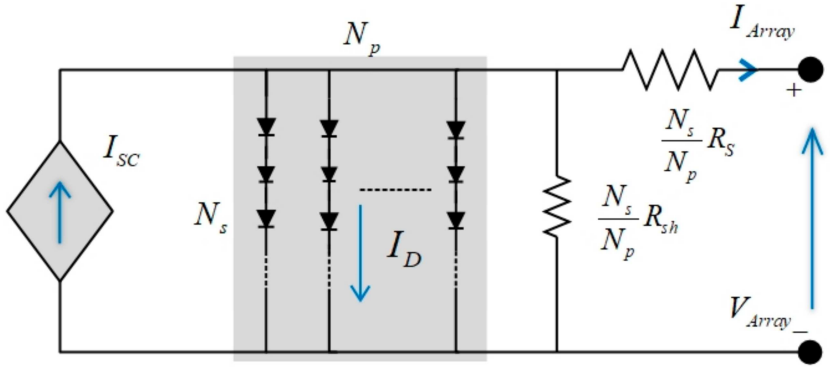

Figure 2. The equivalent of a PV circuit of an array.

The mathematical representation of the PV array [3] is given in Equation (1).

$$I_{Array} = N_p I_{SC} - N_p I_D \left[\exp\left(\frac{V_{Array} + I_{Array} \frac{N_s}{N_p} R_S \, (q)}{n V_T N_s} \right) - 1 \right] - \frac{V_{Array} + I_{Array} \frac{N_s}{N_p} R_S}{\frac{N_s}{N_p} R_{Sh}} \quad (1)$$

where I_{Array} is the output current (A); V_{Array} is the voltage (V) of array; I_{SC} solar cell photocurrent (A), where I_D is a solar cell diode reverse saturation current (A); RS is the series resistance (Ω); RP the parallel resistance (Ω); Array is the idealist factor of the p–n junction solar cell diode (value 1–5); nVT represents the thermal voltage (V) depending on the module temperature as $V_T = k \times T_C / q$, where TC solar cell operating temperature (K); q is the electron charge 1.6×10^{-19} C; and k is the Boltzmann's constant 1.38×10^{-23} j/k.

Simulation and representation were based on the Solarex MSX60 PV module comprising 36 polycrystalline cells with in-series linking [3,17,18], as shown in Table 1.

An I–V curve is generally used to identify the outputs of single-diode PV [2]. Generally, to show the PV performance characteristics, there are five key parameters: short-circuit current (I_{SC}); open-circuit voltage (V_{OC}); current at the MPP (I_{mpp}); the voltage at the MPP (V_{mpp}); and power at the MPP (P_{mpp}). The study of the mismatch due to non-uniform aging is illustrated in the following sections.

Table 1. Parameters for the [MSX60] Solarex photovoltaic module at 1000 W/m^2.

Parameter	Value	Units	Symbols
Open-circuit voltage	21.10	V	V_{OC}
Short-circuit current	3.8	A	I_{SC}
MPP power	60	W	P_{mpp}
MPP current	3.5	A	I_{mpp}
MPP voltage	17.10	V	V_{mpp}
Cell temperature	25	°C	T

3. The Offline Reconfiguration Strategy without Replacing Extremely Aged Modules

According to the authors of [7,19], the short-circuit current (I_{SC}) varies more than the open-circuit voltage (V_{OC}) when a PV cell reaches an aging experiment, due to the p–n junction qualities of the cell. This work assessed the aging status of the PV module based on the I_{SC} while keeping the V_{OC} unchanged for various aging conditions. Furthermore, it is believed that uniform aging is experienced by each of the cell units in the same PV module, so the entire PV module can be characterized by a single maximum I_{SC} of each of the cell units. In the case of in-series PV modules forming a PV array, their output currents will be the same, while the total voltages of the module are applied to obtain the output voltage [7].

In the long service time, the non-uniform aging of a PV array is a well-known phenomenon that results from dust, water corrosion, and shadow [3,20]. An example of enhancement in aging and the global maximum power point (GMPP) is illustrated in Figure 3. Regarding aging improvement, it is important to change the PV modules' position based on the aging information. Once rearranged, the characteristic of the PV array output can still involve multi-maximum power points. GMPP refers to the algorithm that determines the global maximum power point. Furthermore, the PV module parameters were as shown in Table 2. To determine the aging condition, the modules were covered using a plastic membrane in Figure 3a,b. Furthermore, the pre-rearrangement 10 × 10 PV array GMPP was 3.969-kW in a medium condition as shown in Table 3, while the post-rearrangement of the array GMPP was 4.2 kW, as shown in Figures 3 and 4a. There was a 5.7% improvement in the entire array efficiency when the array's working end was the GMPP (Figure 3a). Hence, the proposed aging array rearrangement complements the GMPP.

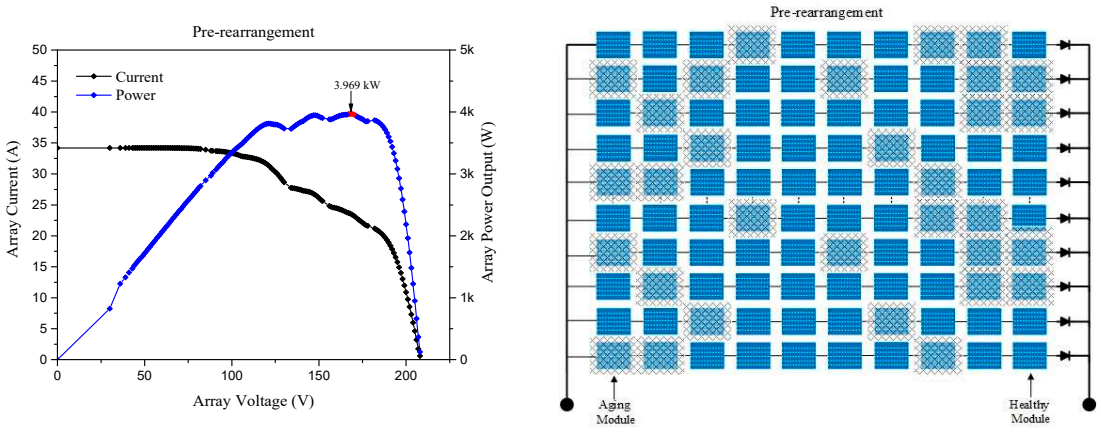

(**a**) (**b**)

Figure 3. The output result for the 10 × 10 PV array. (**a**) PV array without rearrangement. (**b**) The aging modules were covered with a plastic cap for clarification.

Table 2. PV array 10 × 10 parameters before arrangements.

Pre-Arrangement									
0.9 p.u.	0.9 p.u.	0.9 p.u.	0.4 p.u.	0.9 p.u.	0.9 p.u.	0.6 p.u.	0.9 p.u.	0.8 p.u.	0.9 p.u.
0.6 p.u.	0.9 p.u.	0.5 p.u.	0.9 p.u.	0.9 p.u.	0.8 p.u.	0.9 p.u.	0.9 p.u.	0.6 p.u.	0.8 p.u.
0.9 p.u.	0.8 p.u.	0.9 p.u.	0.9 p.u.	0.9 p.u.	0.9 p.u.	0.9 p.u.	0.9 p.u.	0.8 p.u.	0.8 p.u.
0.9 p.u.	0.9 p.u.	0.8 p.u.	0.9 p.u.	0.9 p.u.	0.9 p.u.	0.7 p.u.	0.9 p.u.	0.9 p.u.	0.9 p.u.
0.5 p.u.	0.6 p.u.	0.9 p.u.	0.9 p.u.	0.9 p.u.	0.9 p.u.	0.9 p.u.	0.7 p.u.	0.9 p.u.	0.9 p.u.
0.9 p.u.	0.9 p.u.	0.9 p.u.	0.4 p.u.	0.9 p.u.	0.9 p.u.	0.9 p.u.	0.8 p.u.	0.5 p.u.	0.9 p.u.
0.6 p.u.	0.9 p.u.	0.9 p.u.	0.9 p.u.	0.9 p.u.	0.8 p.u.	0.9 p.u.	0.9 p.u.	0.6 p.u.	0.8 p.u.
0.9 p.u.	0.8 p.u.	0.9 p.u.	0.9 p.u.	0.9 p.u.	0.9 p.u.	0.9 p.u.	0.9 p.u.	0.8 p.u.	0.8 p.u.
0.9 p.u.	0.9 p.u.	0.8 p.u.	0.9 p.u.	0.9 p.u.	0.9 p.u.	0.7 p.u.	0.9 p.u.	0.9 p.u.	0.9 p.u.
0.4 p.u.	0.6 p.u.	0.9 p.u.	0.9 p.u.	0.9 p.u.	0.9 p.u.	0.9 p.u.	0.7 p.u.	0.9 p.u.	0.9 p.u.

Table 3. PV array 10 × 10 parameters after arrangements.

Post-Arrangement									
0.9 p.u.	0.9 p.u.	0.9 p.u.	0.4 p.u.	0.8 p.u.	0.9 p.u.	0.9 p.u.	0.9 p.u.	0.9 p.u.	0.8 p.u.
0.9 p.u.	0.9 p.u.	0.9 p.u.	0.4 p.u.	0.9 p.u.	0.7 p.u.	0.9 p.u.	0.9 p.u.	0.9 p.u.	0.9 p.u.
0.9 p.u.	0.4 p.u.	0.7 p.u.	0.9 p.u.	0.8 p.u.	0.9 p.u.	0.9 p.u.	0.9 p.u.	0.8 p.u.	0.6 p.u.
0.9 p.u.	0.5 p.u.	0.5 p.u.	0.8 p.u.	0.9 p.u.	0.9 p.u.	0.9 p.u.	0.9 p.u.	0.9 p.u.	0.9 p.u.
0.9 p.u.	0.8 p.u.	0.9 p.u.	0.6 p.u.	0.9 p.u.	0.9 p.u.	0.9 p.u.	0.9 p.u.	0.9 p.u.	0.9 p.u.
0.9 p.u.	0.9 p.u.	0.9 p.u.	0.6 p.u.	0.9 p.u.	0.9 p.u.	0.8 p.u.	0.9 p.u.	0.8 p.u.	0.8 p.u.
0.9 p.u.	0.9 p.u.	0.4 p.u.	0.9 p.u.	0.9 p.u.	0.9 p.u.	0.6 p.u.	0.8 p.u.	0.9 p.u.	0.9 p.u.
0.9 p.u.	0.9 p.u.	0.7 p.u.	0.9 p.u.	0.8 p.u.	0.9 p.u.	0.9 p.u.	0.8 p.u.	0.9 p.u.	0.5 p.u.
0.9 p.u.	0.9 p.u.	0.9 p.u.	0.9 p.u.	0.9 p.u.	0.9 p.u.	0.7 p.u.	0.6 p.u.	0.9 p.u.	0.9 p.u.
0.8 p.u.	0.9 p.u.	0.9 p.u.	0.9 p.u.	0.9 p.u.	0.9 p.u.	0.8 p.u.	0.6 p.u.	0.9 p.u.	0.6 p.u.

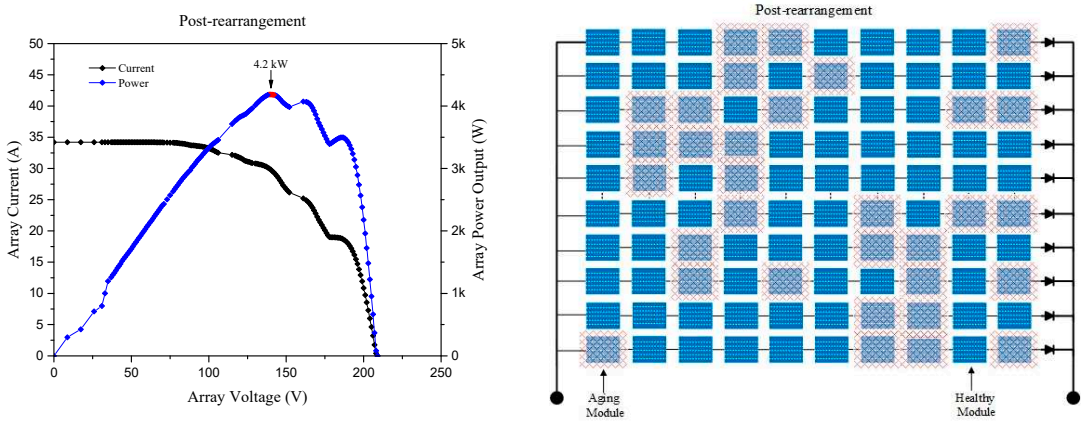

(**a**) (**b**)

Figure 4. The output result for the 10 × 10 PV array. (**a**) PV array with the rearrangement. (**b**) The aging modules were covered with a plastic cap for clarification.

To enhance the effective service time, two important steps should be followed. First is the PV array fault diagnosis and second is the PV array reconfiguration. PV array fault diagnosis involves four well-known methods: thermal camera [21], time-domain reflectometry (TDR) [19,22], applying voltage/current sensors, and earth capacitance measurement (ECM) [22]. The thermal imaging camera can adapt to the non-uniform temperature distribution of the faulty PV array to locate the defective PV module in the background of the online application [23]. The disconnection of the PV modules can be located using an ECM, and the degradation of the PV arrays can be calculated using a TDR. However, ECM as well as TDR can only be utilized in an offline fault diagnosis [21]. Power loss analysis is recommended concerning scale PV array fault diagnosis [24,25]. To reconfigure the PV array, [26,27] provided an example for small-scale reconfiguration. The authors in [9] suggested a classical optimization algorithm (COA) for reconfiguring (RTCT) reconfigurable total cross-tied arrays. To minimize costs, a gene evaluation algorithm (GEA) was applied as the COA requires strong computational effort.

Furthermore, in small-scale PV arrays, the look-up table method has been developed, which cannot be used effectively for large PV arrays [28]. [5] generated a thorough search algorithm [4] devised (sorting algorithm) according to the best and worst paradigm to make the selection of a configuration faster. The fuzzy logical algorithm was also suggested in [29] for identifying the best reconfiguration. Additionally, [5] summarized the most effective online reconfiguration concerning the PV array. However, no reports on large-scale PV array reconfiguration are available. PV array reconfiguration is currently mainly used by relay networks that need a large number of relays and have a high device cost. In terms of large-scale PV arrays, the only viable option for reconfiguring PV is to swap PV modules offline by human labor. An example of such a solution is presented in Figures 5 and 6).

Before flawed PV modules are substituted at higher financial costs, reorganization of such modules can be undertaken via a remedial measure following the identification of the PV array aging map. A variety of reconfiguration strategies are available in the case of PV arrays of large scale, differing in terms of the duration of line reconnection and wiring distances, which determine how efficient and expensive each strategy is. Reconfiguration cost modeling is important for establishing the best reconfiguration strategy. To minimize complexity, the number of reconfigured panels can be used to estimate that cost.

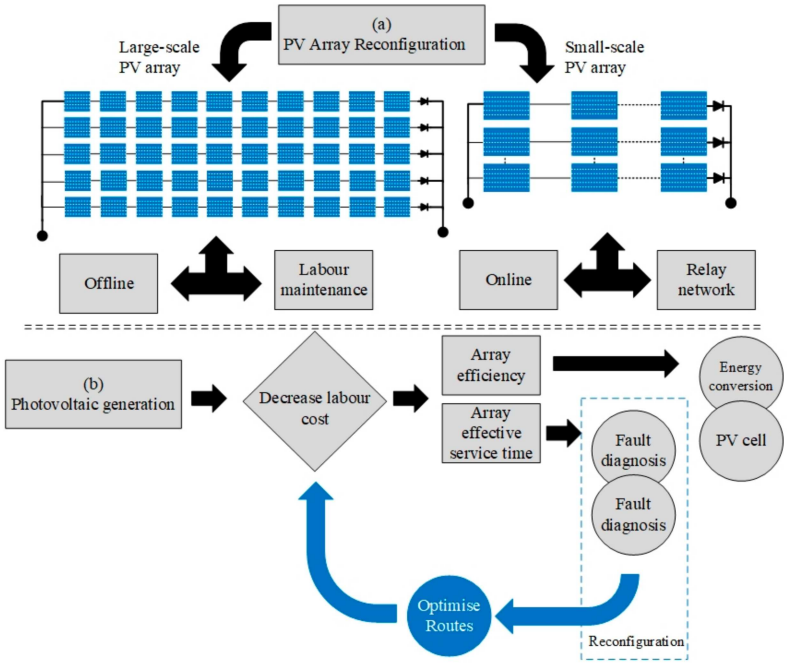

Figure 5. PV array reconfiguration considering the labor cost.

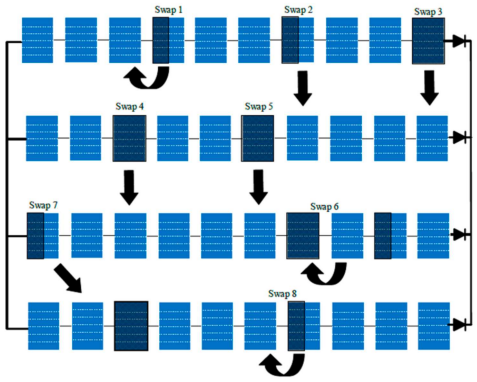

Figure 6. An example of the offline reconfiguration to swap PV modules through human labor in location.

4. Photovoltaic Array Reconfiguration Optimization Scheme

4.1. Reconfiguration Based on Gene Evolution Algorithm (GEA)

The configuration generating the highest power out of all potential connection patterns with the smallest number of PV module substitutions can be identified based on GEA. This algorithm is advantageous because it can undertake a local arbitrary search to some extent and mutation processes can speed up the convergence to an improved solution when the iteration is near an improved solution for a given number of times; moreover, it hinders precocity by affording multiple practical solutions. GEA application requires representation of every configuration based on a row of numbers acting as a chromosome and calculation of the power produced by every configuration based on a fitness function. Pre-prepared chromosomes constitute the fitness function inputs. Subsequently, the GEA relies on the fitness function outputs to determine the chromosomes to be chosen as parents

for the future generation of chromosomes [3]. This necessitates on and off switching of the GEA-computed PV array module as well as the smallest number of substitutions.

$$pv_i = \frac{pv_w}{\sum_{j=1}^{n_{pv}} s_{n(j)} v_{OC}} \qquad \mathrm{j} = 1, 2, 3, \ldots, \mathrm{nm} \tag{2}$$

The GEA consists of the following steps:

- Creation of the fitness function as a normalized quantity: the suggested fitness function is expressed by Equation (2), as follows in Figure 7 and the GEA is intended to increase the pv_i value to the maximum;
- Parametric design underpinned by three conditions, namely, a population size of 300, a chromosome length of n*m, and number of evolution times of 3000;
- Decimal-based encoding approach: direct encoding with the PV module number; thus, chromosome expression can take the form of a sequence $\{1, 2, 3, \ldots, \mathrm{nm}\}$;
- Fitness assessment of all chromosomes in the population: after chromosome conversion into a two-dimensional array (n*m), pv_i calculation is undertaken based on the formulated fitness function;
- Appraisal to achieve iterations or optimization aim: steps 6–8 can be bypassed only if appraisal succeeds;
- Choice of parents for the future generation: this involves sorting the fitness from large to small to choose the surviving chromosomes, followed by arbitrary selection of individuals surviving despite small fitness;
- Parental chromosome crossbreeding: this issue is challenging due to the cross-over approach; the order cross-over technique is employed in the case of the direct use of the point cross, which will cause problems of PV-model duplication and omission in the offspring chromosomes; two hybridization points are chosen arbitrarily between the parents by the sequential hybridization algorithm, with subsequent exchange of hybridization segments and the relative locations of the parental models help to establish the other locations; for example, the chromosome can be given as the sequence $\{1, 2, \ldots, 10\}$.

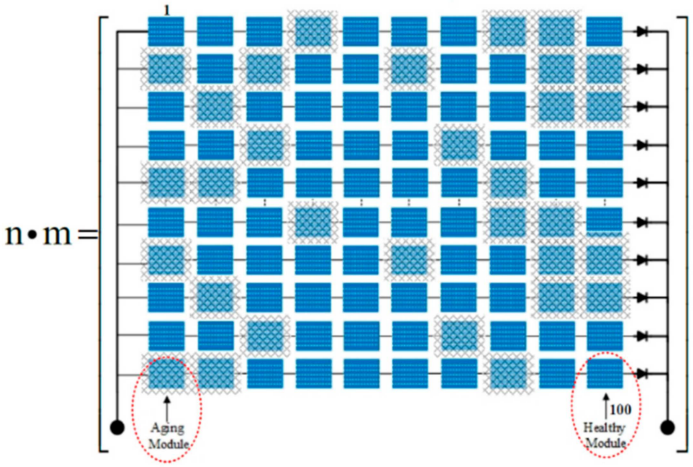

Figure 7. The first step of the reconfiguration algorithm (before arrangement).

Suppose: Parent one = {10, 8, 6, 3, 7, 4, 1, 5, 9, 2} and Parent two = {1, 5, 10, 6, 9, 8, 2, 4, 3, 7}. Then, the random hybridization points are 4 and 7.

As expressed:

- ❖ Parent one = {10, 8, 6, 3, | 7, 4, 1, 5, |, 9, 2}
- ❖ Parent two = {1, 5, 10, 6, | 9, 8, 2, 4, |, 3, 7}.

In order to swap the hybrids, first

- ❖ Parent one' = {#, #, #, #, | 9, 8, 2, 4, |, #, #}
- ❖ Parent two'= {#, #, #, #, | 7, 4, 1, 5, |, #, #}.

Then, start from the second crossbreeding point of one of the parents, get to the group {9, 2, 10, 8, 6, 3, 7, 4, 1, 5}; then remove the elements in the crossbreeding {9, 8, 2, 4}, finally accessing the {10, 6, 3, 7, 1, 5}.

Finally, coordinate the hybridization point 7 filled in the parent one':

- ❖ Parent one' = {3, 7, 1, 5, | 9, 8, 2, 4,|, 10, 6}, from the second crossing point in turn.

Similarly:

- ❖ Parent two' = {4, 9, 10, 2, | 7, 3, 1, 6,|, 8, 5}.

- Chromosomal mutation: this helps to both diversify the population and to ensure universal optimization; the particular rate of mutation for the chosen mutant individual is the basis for the arbitrary selection of three integers that meet the condition 1 < u < v < w < n*m and the genes between *v* and *u* including u and *v*, with paragraph insertion after w; the fourth step is subsequently undertaken;
- Optimal output chromosome: comparative analysis between every configuration satisfying every step and the initial configuration is shown in Figure 8.

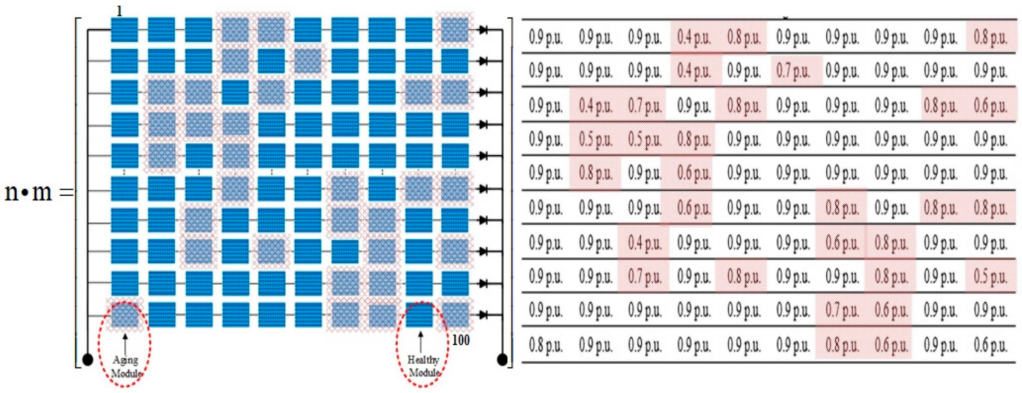

Figure 8. The final step of the reconfiguration algorithm (after arrangement).

Nine iterations were enough to obtain the ideal reconfiguration for a 10 × 10 PV array with heterogeneous aging. Figure 9 shows this in the final step, alongside the smallest number of swap times and the highest amount of output power. Python 3.8.2 Intel (R) Core (7M) i7-8565u CPU @1.80 GHZ/windows 10/8 GB/512gb SSD/UHD 620 is suitable for determining the best configuration for a sizable PV array. For the purposes of direct comparative analysis, the PV arrays, pre- and post-reconfiguration, are illustrated in Figures 7 and 8.

Identification of the ideal reconfiguration made it possible to reach the last step by enhancing the output power and reducing the number of swap times as much as possible. The factors that need to be considered in assessing the cost of reconfiguration are discussed below.

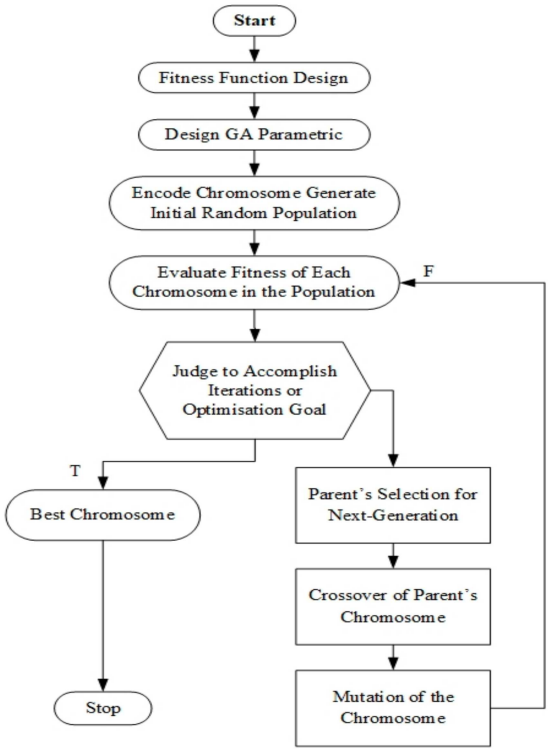

Figure 9. Displayed the flow chart of Gene Evolution Algorithm (GEA) procedure of PV array reconfiguration.

4.2. Cost Analysis of Rearrangements for PV Array

According to the survey, the PV array is assumed to need to be rebuilt on average once a year, and the PV array will produce 8 h of power per day. To swap panels from one position to another, a professional grid worker requires an average of 45 mints and 30 mints to install a new module [30].

Some criteria need to be identified to explain the economic benefit work outlined below for the aging PV collection:

- PV_{pre} is the PV array output power before arrangements
- PV_{post} is the output power after arrangements
- A_e is the additional electricity
- H_w is the average hourly wage of the manpower (60 min)
- E_p is the electricity price
- N_s is the number of swaps/replace
- T_s is the time per swap/replace
- C_{per} is the cost per swap/replace
- C_{sawp} is the cost of swaps
- $C_{replace}$ is the cost of replace
- Wt_{Cost} is the cost per watt peak (cents/Wp)
- S_s is the size per module (Wp)
- *USD* is United States Dollar ($)

$$\text{PV array output difference } A_e = PV_{post} - PV_{pre} \tag{3}$$

Next, equations are subject to swap PV modules:

$$\text{Compute the cost per swap } C_{per} = \frac{45}{H_w} \times T_s \tag{4}$$

$$\text{Compute the cost of swap } C_{swap} = C_{per} \times N_s \tag{5}$$

Here, equations are subject to replace PV modules:

$$\text{Compute the cos t per replace } C_{per} = \frac{30}{H_w} \times T_s \tag{6}$$

$$\text{Compute the cos t of replace } C_{replace} = (N_s \times New\ pnael) + (N_s \times C_{per}) \tag{7}$$

The total economic benefit in the next equations from swap/replace:

$$\text{A year electric revenue } A_e \times 8 \times 365 \times year \times E_p - C_{swap/replace} \tag{8}$$

$$\text{Total electric revenue} = \text{ A year electric revenue} \times 10 \text{ years} \tag{9}$$

The cost-effectiveness of the topology reconstruction technique for PV arrays was validated by considering 2020 as the PV system benchmark, the average cost of electricity price, average handling cost associated with PV panel replacement, and average labor cost in various countries [31–34]. Table 4 outlines these aspects.

Table 4. Electricity price and labor cost in 2020.

Country	Electricity Prices $/kWh	Hourly Wage $/hr	Cost Per Swap $/time	Cost Per Replace $/time
Saudi Arabia	0.059	7.98	5.98	3.99
Pakistan	0.108	1.42	1.07	0.71
India	0.097	1.19	0.89	0.60
France	0.177	24.87	18.65	12.44
United Kingdom	0.242	17.2	12.9	8.60
Germany	0.301	27.91	20.93	13.96
Greece	0.179	8.28	6.21	4.14
Cyprus	0.263	7.11	5.21	3.56
Jamaica	0.219	1.24	0.93	0.62
China	0.091	9.57	7.17	4.79
Japan	0.249	26.33	19.74	13.17
Australia	0.227	33.35	25.02	16.68
Brazil	0.127	6.05	4.54	3.03
US states	0.126	15.47	11.8	7.78

The following part explores two cases regarding the economic advantages pre- and post-arrangements of the proposed method.

5. Case Studies and Simulation Results

The suggested algorithm was verified by the random generation of heterogeneous aging factors for 10 × 10 PV arrays. MATLAB Intel (R) Core (7M) i7-8565u CPU @1.80 GHZ/windows 10/8 GB/512GB SSD/UHD 620 was used to assemble a PV array model to calculate the highest possible power outputs that such PV configurations would be capable of, both before and after =intervention. The 10 × 10 PV arrays were established to have equivalent computing times of 18-kW and 43-kW, respectively.

5.1. Case 1 (Arrange Aging Modules of 10 × 10 PV Array)

Under typical test conditions of 1000 W/m2 irradiance and 25 °C module temperature, a normal module has a maximum short-circuit current of 1 p.u. (STC). Table 5 shows a standard large-scale PV array with heterogeneous aging, which serves as a testing branch, with every number denoting the highest aging-related output power. As is conventional for PV arrays available on the market, every string contains PV modules within a series connection, while the strings have a parallel connection (SP). Furthermore, the aging factors are in the spectrum of 0.9–0.4 p.u. (Table 5), so the plotting of the I–V and P–V curves was undertaken as shown in Figure 10a,b, with the suggested algorithm enabling output power

enhancement of 3.87% for the 18-kW 10 × 10 PV array and 1.76% for the 43-kW 10 × 10 PV array, respectively. The increase in power was reflected by the fact that the mean average computation time was 0.129375 s.

Table 5. The parameters associated with the two types of 10 × 10 PV arrays (i.e., 18-kW and 43-kW) after application of reconfiguration in 14 different countries.

Pre-Arrangement									
0.9 p.u.	0.9 p.u.	0.9 p.u.	0.4 p.u.	0.9 p.u.	0.9 p.u.	0.6 p.u.	0.9 p.u.	0.8 p.u.	0.9 p.u.
0.6 p.u.	0.9 p.u.	0.5 p.u.	0.9 p.u.	0.9 p.u.	0.8 p.u.	0.9 p.u.	0.9 p.u.	0.6 p.u.	0.8 p.u.
0.9 p.u.	0.8 p.u.	0.9 p.u.	0.9 p.u.	0.9 p.u.	0.9 p.u.	0.9 p.u.	0.9 p.u.	0.8 p.u.	0.8 p.u.
0.9 p.u.	0.9 p.u.	0.8 p.u.	0.9 p.u.	0.9 p.u.	0.9 p.u.	0.7 p.u.	0.9 p.u.	0.9 p.u.	0.9 p.u.
0.5 p.u.	0.6 p.u.	0.9 p.u.	0.9 p.u.	0.9 p.u.	0.9 p.u.	0.9 p.u.	0.7 p.u.	0.9 p.u.	0.9 p.u.
0.9 p.u.	0.9 p.u.	0.9 p.u.	0.4 p.u.	0.9 p.u.	0.9 p.u.	0.9 p.u.	0.8 p.u.	0.5 p.u.	0.9 p.u.
0.6 p.u.	0.9 p.u.	0.9 p.u.	0.9 p.u.	0.9 p.u.	0.8 p.u.	0.9 p.u.	0.9 p.u.	0.6 p.u.	0.8 p.u.
0.9 p.u.	0.8 p.u.	0.9 p.u.	0.9 p.u.	0.9 p.u.	0.9 p.u.	0.9 p.u.	0.9 p.u.	0.8 p.u.	0.8 p.u.
0.9 p.u.	0.9 p.u.	0.8 p.u.	0.9 p.u.	0.9 p.u.	0.9 p.u.	0.7 p.u.	0.9 p.u.	0.9 p.u.	0.9 p.u.
0.4 p.u.	0.6 p.u.	0.9 p.u.	0.9 p.u.	0.9 p.u.	0.9 p.u.	0.9 p.u.	0.7 p.u.	0.9 p.u.	0.9 p.u.
Post-Arrangement									
0.9 p.u.	0.9 p.u.	0.9 p.u.	0.4 p.u.	0.8 p.u.	0.9 p.u.	0.9 p.u.	0.9 p.u.	0.9 p.u.	0.8 p.u.
0.9 p.u.	0.9 p.u.	0.9 p.u.	0.4 p.u.	0.9 p.u.	0.7 p.u.	0.9 p.u.	0.9 p.u.	0.9 p.u.	0.9 p.u.
0.9 p.u.	0.9 p.u.	0.7 p.u.	0.9 p.u.	0.8 p.u.	0.9 p.u.	0.9 p.u.	0.9 p.u.	0.8 p.u.	0.6 p.u.
0.9 p.u.	0.5 p.u.	0.5 p.u.	0.8 p.u.	0.9 p.u.	0.9 p.u.	0.9 p.u.	0.9 p.u.	0.9 p.u.	0.9 p.u.
0.9 p.u.	0.8 p.u.	0.9 p.u.	0.6 p.u.	0.9 p.u.	0.9 p.u.	0.9 p.u.	0.9 p.u.	0.9 p.u.	0.9 p.u.
0.9 p.u.	0.9 p.u.	0.9 p.u.	0.6 p.u.	0.9 p.u.	0.9 p.u.	0.8 p.u.	0.9 p.u.	0.8 p.u.	0.8 p.u.
0.9 p.u.	0.9 p.u.	0.4 p.u.	0.9 p.u.	0.9 p.u.	0.9 p.u.	0.6 p.u.	0.8 p.u.	0.9 p.u.	0.9 p.u.
0.9 p.u.	0.9 p.u.	0.7 p.u.	0.9 p.u.	0.8 p.u.	0.9 p.u.	0.9 p.u.	0.8 p.u.	0.9 p.u.	0.5 p.u.
0.9 p.u.	0.9 p.u.	0.9 p.u.	0.9 p.u.	0.9 p.u.	0.9 p.u.	0.7 p.u.	0.6 p.u.	0.9 p.u.	0.9 p.u.
0.8 p.u.	0.9 p.u.	0.9 p.u.	0.9 p.u.	0.9 p.u.	0.9 p.u.	0.8 p.u.	0.6 p.u.	0.9 p.u.	0.6 p.u.

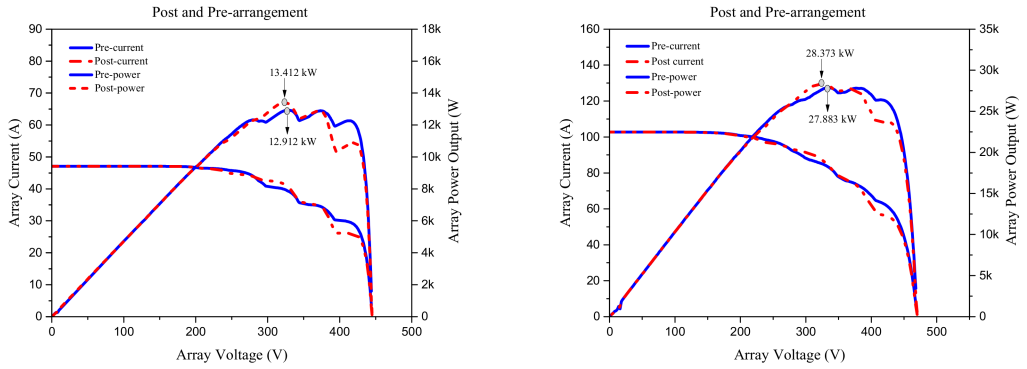

Figure 10. The outputs associated with the two types of 10 × 10 PV arrays, namely, 18-kW (**a**) and 43-kW (**b**) before and after the implementation of reconfiguration.

5.1.1. Scenario One (Initial–Final Rates Return of Electricity Revenue)

Figure 10a,b illustrates the output power enhancement in the case of a 10 × 10 PV array. At the same time, Table 5 details the outcomes of the simulation based on the cost of electric power and labor in fourteen countries necessitating forty-four manual swap times. Table 6 indicates the initial and final rate returns of electric revenue for the two types of 10 × 10 PV arrays (i.e., 18-kW and 43-kW), without taking into account the most remarkable economic advantage. Thus, in the case of the 18-kW 10 × 10 PV array, the post-reconfiguration electric revenue increased by 3.87%, while in the case of the 43-kW array, the increase achieved by the suggested approach was 1.76%, according to Table 6.

Table 6. The original and final rate returns of electric revenue associated with the two types of 10 × 10 PV arrays, without taking into account the greatest annual economic advantage.

Country	Initial Rate Return of Electric Revenue 18-kW ($)	Final Rate Return of Electric Revenue 18-kW ($)	Initial Rate Return of Electric Revenue 43-kW ($)	Final Rate Return of Electric Revenue 43-kW ($)
Saudi Arabia	17,795.83	18,484.95	33,625.78	34,216.7
Pakistan	4071.93	4229.61	8793.18	8947.71
India	3657.19	3798.81	7897.58	8036.37
France	46,714.07	48,523.01	100,877.35	102,650.11
United Kingdom	36,496.54	37,909.82	78,812.97	80,197.99
Germany	56,743.08	58,940.38	122,534.63	124,687.99
Greece	20,246.53	21,030.55	43,721.66	44,490.01
Cyprus	19,831.8	20,599.76	42,826.06	43,578.66
Jamaica	8256.97	8576.71	17,830.62	18,143.97
China	17,154.88	17,819.18	44,454.42	45,235.64
Japan	46,940.28	48,757.98	121,639.03	12,3776.65
Australia	59,910.13	62,230.07	147,855.74	150,454.07
Brazil	14,364.86	14,921.12	31,020.4	31,565.53
US states	28,503.5	29,607.26	71,810.99	73,072.96

5.1.2. Scenario Two (Net Profits of Additional Electric Revenue)

Regarding the cost of high labor and low electricity price in some countries, Table 7 and Equation (5) reflect that, by reducing the number of swap times, the suggested approach can make the offline reconfiguration more cost-effective, whilst also significantly enhancing overall profit (Table 8). However, it is unclear how the process benefits profitability in countries where labor price is high, but the electricity price is low, in which case the labor cost can be diminished. Still, the electric revenue profit cannot be increased.

Table 7. Assessment of economic advantages taking into account minimum handling times.

Country	Cost of Swapping 44 Modules $/time	Best Cost-Effective Maintenance Period Time	Additional Electric Revenue 18-kW ($)	Cost of Swapping 44 Modules $/time	Best Cost-Effective Maintenance Period Time	Additional Electric Revenue 43-kW ($)
Saudi Arabia	263.34	8	607.9	263.34	7	327.58
Pakistan	46.86	1	110.82	46.86	1	107.67
India	39.27	1	102.35	39.27	1	99.52
France	820.71	7	988.23	820.71	7	952.05
United Kingdom	567.60	4	845.68	567.60	4	817.41
Germany	921.03	5	1276.27	921.03	5	1232.32
Greece	273.24	3	510.78	273.24	3	495.10
Cyprus	234.63	2	533.33	234.63	2	517.97
Jamaica	40.92	1	278.82	40.92	1	272.43
China	315.81	5	348.49	315.81	6	465.41
Japan	868.89	5	948.81	868.89	6	1268.73
Australia	1100.55	7	1219.39	1100.55	8	1497.78
Brazil	199.65	3	356.61	199.65	3	345.48
US states	510.51	6	593.25	510.51	7	751.46

Table 8. The original and final rate returns of electric revenue associated with the two types of 10 × 10 PV arrays, taking into account the greatest annual economic advantage.

Country	The Initial Value of Electric Revenue without Considering Labor Cost 18-kW ($)	Net Profit of Final Value Electric Revenue by Considering Labor Cost 18-kW ($)	The Initial Value of Electric Revenue without Considering Labor Cost 43-kW ($)	Net Profit of Final Value Electric Revenue by Considering Labor Cost 43-kW ($)
Saudi Arabia	17,795.83	18,221.61	33,625.78	33,953.36
Pakistan	4071.93	4182.75	8793.18	8900.85
India	3657.19	3759.54	7897.58	7997.1
France	46,714.07	47,702.3	100,877.35	101,829.4
United Kingdom	36,496.54	37,342.22	78,812.97	79,630.39
Germany	56,743.08	58,019.35	122,534.63	123,766.96
Greece	20,246.53	20,757.31	43,721.66	44,216.77
Cyprus	19,831.8	20,365.13	42,826.06	43,344.03
Jamaica	8256.97	8535.79	17,830.62	18,103.05
China	17,154.88	17,503.37	44,454.42	44,919.83
Japan	46,940.28	47,889.09	121,639.03	122,907.76
Australia	59,910.13	61,129.52	147,855.74	149,353.52
Brazil	14,364.86	14,721.47	31,020.4	31,365.88
US states	28,503.5	29,096.75	71,810.99	72,562.45

The outcomes of the simulation are presented in Table 8. It can be seen that manual swap had to be performed forty-four times, according to the costs associated with electricity and labor force in the fourteen countries that were examined. The suggested algorithm considered one decade following PV module installation was used to determine the most remarkable economic advantage. Meanwhile, Table 7 indicates the extra electric revenue profit made possible by the (18-kW and 43-kW) PV array and the associated cost of labor, the calculation of which was undertaken based on Equations (3)–(9). Furthermore, the proportion of net electric revenue profit achieved after the reconfiguration was carried out based on the suggested approach is provided in Figure 11.

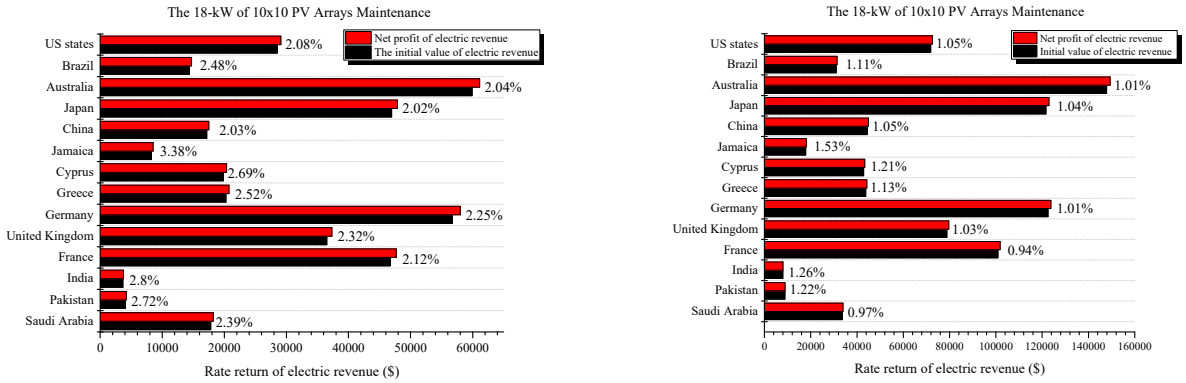

Figure 11. The increase in rate returns of electric revenue associated with the two types of 10 × 10 PV arrays, taking into account the greatest annual economic advantage.

In order to achieve the maximum net profit return, the suggested algorithm yielded a particular maintenance time in each case. This explains the discrepancies that have been noted concerning maintenance times. To give an example, the algorithm indicated that, in countries like Pakistan, India, and Jamaica, maintenance could be carried out in the first year to achieve a net profit from the electric revenue due to the high cost of electricity, but low labor cost. On the other hand, the algorithm indicated that maintenance could be conducted in the second year in countries like Cyprus to attain a better net profit from electric revenue. In contrast, maintenance could be conducted in the third year in Greece and Brazil and in the fourth year in the case of the UK to benefit net profit. Furthermore, maintenance can be carried out in the fifth year in Germany, China, and Japan, and in the sixth year in the U.S. Moreover, the increase in electric revenue profit in France and Australia could be enhanced by undertaking maintenance in the seventh year after PV installation, according to the suggested algorithm. Finally, the algorithm indicated that in a country like Saudi Arabia, maintenance can be carried out in year eight to achieve a net profit from the electric revenue due to the low cost of electricity, but high labor cost. Figure 12 illustrates the increase in electric revenue.

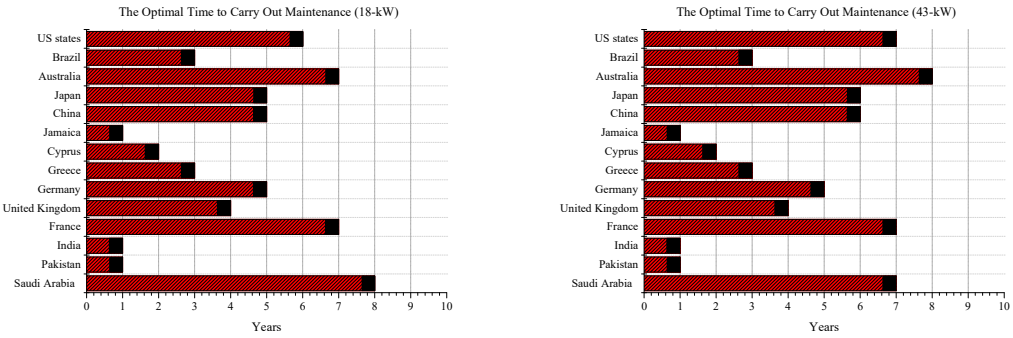

Figure 12. The year identified by the suggested algorithm as the optimal time to carry out maintenance in order to achieve the greatest economic advantage.

5.2. Case 2 (Combine Swap/Replace Aging Modules of 10 × 10 PV Array)

In relation to the second case that was explored, the outcomes produced by the assessment of the maintenance costs associated with the two types of PV arrays served as the basis for reaching a conclusion with regard to the extent to which the profit from the electric revenue could be increased to enhance the economic advantages in the fourteen countries that were considered in Table 9. Furthermore, as indicated in Table 10, related to the conditions before reconfiguration, aging factors in the range of (0.9–0.4 p.u.) and lacking homogeneity were produced arbitrarily for a 10 × 10 PV array of large scale, which consisted of ten strings within a parallel connection and ten modules within a series

connection. Once the aging factors were identified in the PV array, it was necessary to undertake the substitution of the aged PV panel with a new PV panel (1 p.u.). In other words, substitution is required in the case of all aged PV panels with less than 0.6 p.u. The conditions refer to this after reconfiguration in Table 10. Furthermore, Table 10 also shows that when the suggested method was applied, the PV array of 18-kW displayed an enhancement in power of 11.35% after the reconfiguration. The same table revealed that the PV array of 43-kW achieved an enhancement in the power of 10.8% after the reconfiguration. Meanwhile, Figure 13a,b illustrates the plotting of the I–V curve and the P–V curve, which was accomplished in a mean computational time of 0.159364 s. Table 10 lists the parameters that need to be taken into account concerning the costs of electric power and labor in the fourteen countries examined.

Table 9. The PV array 10 × 10 parameter inputs.

Parameters Input	10 × 10 PV Array 18 kW	10 × 10 PV Array 43 kW	Unit
Number of Replace	6	6	PV module
Number of Swap	38	38	PV module
Time per replace	30	30	Minute
Time per swap	45	45	Minute
Cost per panel	40	70	USD
Cost per watt peak	0.22	0.36	Cents/Wp
Size per module	180	430	Wp
Initial Output	12.912	27.883	kW
Final Output	15.957	33.990	kW
Difference	3.045	6.108	kW
Number of Replace	6	6	PV module
Number of Swap	38	38	PV module

Table 10. The parameters associated with the two types of 10 × 10 PV arrays (i.e., 18-kW and 43-kW) after application of reconfiguration in 14 different countries.

Pre-Arrangement									
0.9 p.u.	0.9 p.u.	0.9 p.u.	0.4 p.u.	0.9 p.u.	0.9 p.u.	0.6 p.u.	0.9 p.u.	0.8 p.u.	0.9 p.u.
0.6 p.u.	0.9 p.u.	0.5 p.u.	0.9 p.u.	0.9 p.u.	0.8 p.u.	0.9 p.u.	0.9 p.u.	0.6 p.u.	0.8 p.u.
0.9 p.u.	0.8 p.u.	0.9 p.u.	0.9 p.u.	0.9 p.u.	0.9 p.u.	0.9 p.u.	0.9 p.u.	0.8 p.u.	0.8 p.u.
0.9 p.u.	0.9 p.u.	0.8 p.u.	0.9 p.u.	0.9 p.u.	0.9 p.u.	0.7 p.u.	0.9 p.u.	0.9 p.u.	0.9 p.u.
0.5 p.u.	0.6 p.u.	0.9 p.u.	0.9 p.u.	0.9 p.u.	0.9 p.u.	0.9 p.u.	0.7 p.u.	0.9 p.u.	0.9 p.u.
0.9 p.u.	0.9 p.u.	0.9 p.u.	0.4 p.u.	0.9 p.u.	0.9 p.u.	0.9 p.u.	0.8 p.u.	0.5 p.u.	0.9 p.u.
0.6 p.u.	0.9 p.u.	0.9 p.u.	0.9 p.u.	0.9 p.u.	0.8 p.u.	0.9 p.u.	0.9 p.u.	0.6 p.u.	0.8 p.u.
0.9 p.u.	0.8 p.u.	0.9 p.u.	0.9 p.u.	0.9 p.u.	0.9 p.u.	0.9 p.u.	0.9 p.u.	0.8 p.u.	0.8 p.u.
0.9 p.u.	0.8 p.u.	0.9 p.u.	0.9 p.u.	0.9 p.u.	0.9 p.u.	0.9 p.u.	0.9 p.u.	0.8 p.u.	0.8 p.u.

Table 10. *Cont.*

Pre-Arrangement									
0.9 p.u.	0.9 p.u.	0.8 p.u.	0.9 p.u.	0.9 p.u.	0.9 p.u.	0.7 p.u.	0.9 p.u.	0.9 p.u.	0.9 p.u.
0.4 p.u.	0.6 p.u.	0.9 p.u.	0.9 p.u.	0.9 p.u.	0.9 p.u.	0.9 p.u.	0.7 p.u.	0.9 p.u.	0.9 p.u.
Post-Arrangement									
0.9 p.u.	0.9 p.u.	0.9 p.u.	1 p.u.	0.8 p.u.	0.9 p.u.	0.9 p.u.	0.9 p.u.	0.9 p.u.	0.8 p.u.
0.9 p.u.	0.9 p.u.	0.9 p.u.	1 p.u.	0.9 p.u.	0.7 p.u.	0.9 p.u.	0.9 p.u.	0.9 p.u.	0.9 p.u.
0.9 p.u.	0.9 p.u.	0.7 p.u.	0.9 p.u.	0.8 p.u.	0.9 p.u.	0.9 p.u.	0.9 p.u.	0.8 p.u.	0.6 p.u.
0.9 p.u.	1 p.u.	1 p.u.	0.8 p.u.	0.9 p.u.	0.9 p.u.	0.9 p.u.	0.9 p.u.	0.9 p.u.	0.9 p.u.
0.9 p.u.	0.8 p.u.	0.9 p.u.	0.6 p.u.	0.9 p.u.	0.9 p.u.	0.9 p.u.	0.9 p.u.	0.9 p.u.	0.9 p.u.
0.9 p.u.	0.9 p.u.	0.9 p.u.	0.6 p.u.	0.9 p.u.	0.9 p.u.	0.8 p.u.	0.9 p.u.	0.8 p.u.	0.8 p.u.
0.9 p.u.	0.9 p.u.	1 p.u.	0.9 p.u.	0.9 p.u.	0.9 p.u.	0.6 p.u.	0.8 p.u.	0.9 p.u.	0.9 p.u.
0.9 p.u.	0.9 p.u.	0.7 p.u.	0.9 p.u.	0.8 p.u.	0.9 p.u.	0.9 p.u.	0.8 p.u.	0.9 p.u.	1 p.u.
0.9 p.u.	0.9 p.u.	0.9 p.u.	0.9 p.u.	0.9 p.u.	0.9 p.u.	0.7 p.u.	0.6 p.u.	0.9 p.u.	0.9 p.u.
0.8 p.u.	0.9 p.u.	0.9 p.u.	0.9 p.u.	0.9 p.u.	0.9 p.u.	0.8 p.u.	0.6 p.u.	0.9 p.u.	0.6 p.u.

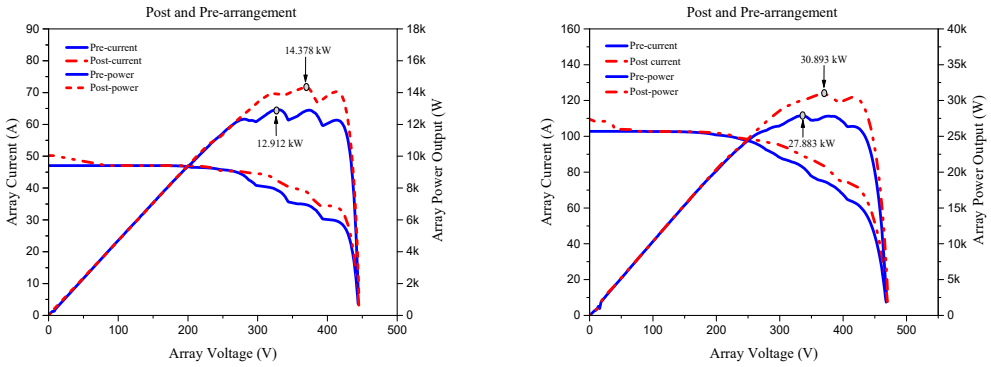

(**a**) (**b**)

Figure 13. The outputs associated with the two types of 10 × 10 PV arrays, namely, 18-kW (**a**) and 43-kW (**b**) before and after the implementation of reconfiguration.

5.2.1. Scenario One (Initial-Final Rates Return of Electricity Revenue)

In the earlier part, the enhancement of the output power associated with the 10 × 10 PV arrays was addressed, and the process is illustrated in Figure 13a,b. The outcomes of the simulation are presented in Table 10. It can be seen that manual swap had to be performed 38 times and manual replacing six times, according to the costs associated with electric power and labor force in the fourteen countries that were examined. Meanwhile, Table 11 provides the initial and final rate returns related to the electric revenue of both the 18-kW

10 × 10 PV array and the 43-kW 10 × 10 PV array, but without taking into account the most significant economic advantage. It can thus be observed that, by comparison to the final rate return of electric revenue, the initial rate return of electric revenue before reconfiguration is lower. This reflects the positive effect of the suggested approach, which determined an 11.35% increase in the electric revenue of the 18-kW 10 × 10 PV array in all of the examined countries following the implementation of reconfiguration. Similarly, the approach also had a favorable impact on the 43-kW 10 × 10 PV array, increasing the related electric revenue by 10.8% in all of the fourteen countries according to Table 11.

Table 11. The original and final rate returns associated with the 18-kW and 43-kW 10 × 10 PV arrays, without taking into account the greatest economic advantage per year.

Country	Initial Rate Return of Electric Revenue 18-kW ($)	Final Rate Return of Electric Revenue 18-kW ($)	Initial Rate Return of Electric Revenue 43-kW ($)	Final Rate Return of Electric Revenue 43-kW ($)
Saudi Arabia	8897.92	9908.17	14,411.05	15,966.74
Pakistan	8143.86	9068.49	17,586.37	19,484.83
India	7314.39	8144.85	15,795.16	17,500.27
France	20,020.31	22,293.38	28,822.1	31,933.48
United Kingdom	18,248.27	20,320.14	19,703.24	21,830.23
Germany	22,697.23	25,274.22	24,506.93	27,152.48
Greece	13,497.69	15,030.19	14,573.89	16,147.15
Cyprus	9915.91	11,041.73	21,413.03	23,724.59
Jamaica	8256.97	9194.44	17,830.62	19,755.46
China	10,292.93	11,461.57	14,818.14	16,417.78
Japan	28,164.17	31,361.87	40,546.34	44,923.36
Australia	25,675.77	28,590.94	36,963.94	40,954.23
Brazil	9576.57	10,663.88	20,680.26	22,912.72
US states	14,251.75	15,869.86	20,517.43	22,732.31

5.2.2. Scenario Two (Net Profits of Additional Electric Revenue)

As can be deduced from Table 12 and Equations (5)–(9) about the costs of labor and electricity price in the investigated countries, the approach put forth in this paper can reduce the number of times that substitutions are performed, thus making offline reconfiguration less expensive. At the same time, this would also determine a significant rise in overall profit (Table 12). On the other hand, there is a lack of clarity about how the approach benefits profitability in countries where labor and electricity price is expensive; in the case of such countries, the cost of labor can be diminished, but the electric revenue profit cannot be increased.

The outcomes of the simulation that are presented in Table 13 point to the fact that manual swap had to be performed thirty-eight times, while substitution had to be performed six replacement times, according to the costs associated with electric power and labor force in the fourteen countries that were examined. Meanwhile, Equations (4)–(10) facilitated the calculation of the extra electric revenue profit associated with the (18-kW and 43-kW) PV array and the equivalent cost of labor. The figures that were thus obtained are given in Table 7. Furthermore, the proportion of the net profit of electric revenue that was achieved following the application of the reconfiguration based on the suggested approach is indicated in Figure 14.

Table 12. The assessment of economic advantage, taking into account the lowest number of times that handling is required.

Country	Cost of Swap/Replace Modules $/Time	Best Cost-Effective Maintenance Period Time	Additional Electric Revenue 18-kW ($)	Cost of Swap/Replace Modules $/Time	Best Cost-Effective Maintenance Period Time	Additional Electric Revenue 43-kW ($)
Saudi Arabia	491.37	4	518.88	671.37	3	884.32
Pakistan	284.73	2	639.91	464.73	2	1433.74
India	277.49	2	552.97	457.49	2	1247.62
France	1023.41	3	1249.66	1203.41	2	1907.97
United Kingdom	781.8	2	1290.07	961.8	1	1165.19
Germany	1119.17	2	1457.83	1299.17	1	1346.38
Greece	500.82	2	1031.68	680.82	1	892.45
Cyprus	463.97	1	661.86	643.97	1	1667.59
Jamaica	279.06	1	658.42	459.06	1	1465.77
China	541.46	3	627.18	721.46	2	878.18
Japan	1069.4	3	2128.3	1249.4	2	3127.63
Australia	1290.53	3	1624.65	1470.53	2	2519.77
Brazil	430.58	2	656.73	610.58	2	1621.88
US states	727.31	3	890.81	907.31	2	1307.57

Table 13. The original and final rate returns associated with the substituting modules of the 10 × 10 PV arrays, taking into account the greatest economic advantage per year.

Country	The Initial Value of Electric Revenue without Considering Labor Cost 18-kW ($)	Net Profit of Final Value Electric Revenue by Considering Labor Cost 18-kW ($)	The Initial Value of Electric Revenue without Considering Labor Cost 43-kW ($)	Net Profit of Final Value Electric Revenue by Considering Labor Cost 43-kW ($)
Saudi Arabia	8897.92	9416.8	14,411.05	15,295.37
Pakistan	8143.86	8783.76	17,586.37	19,020.1
India	7314.39	7867.36	15,795.16	17,042.78
France	20,020.31	21,269.97	28,822.1	30,730.07
United Kingdom	18,248.27	19,538.34	19,703.24	20,868.43
Germany	22,697.23	24,155.06	24,506.93	25,853.31
Greece	13,497.69	14,529.37	14,573.89	15,466.33
Cyprus	9915.91	10,577.76	21,413.03	23,080.62
Jamaica	8256.97	8915.38	17,830.62	19,296.4
China	10,292.93	10,920.11	14,818.14	15,696.32
Japan	28,164.17	30,292.47	40,546.34	43,673.97
Australia	25,675.77	27,300.42	36,963.94	39,483.71
Brazil	9576.57	10,233.3	20,680.26	22,302.15
US states	14,251.75	15,142.56	20,517.43	21,825.01

The analysis that was performed based on the same interval of maintenance applied in the earlier part revealed that suboptimal electric revenue was achieved. This can be attributed to the fact that the substitution of solar panels with new ones in countries like Pakistan, India, and Jamaica is highly expensive. On the other hand, the rate of the electric revenue was medium in the case of the other countries that were analyzed. Thus, it was concluded that, in the case of the latter, maintenance can begin from the second to the fourth year, as indicated in Figure 15. Despite such observations, it can be attested that an approach involving a mixture of PV panel swap and substitution could help to ensure that the performance of midlife maintenance is advantageous in the majority of countries.

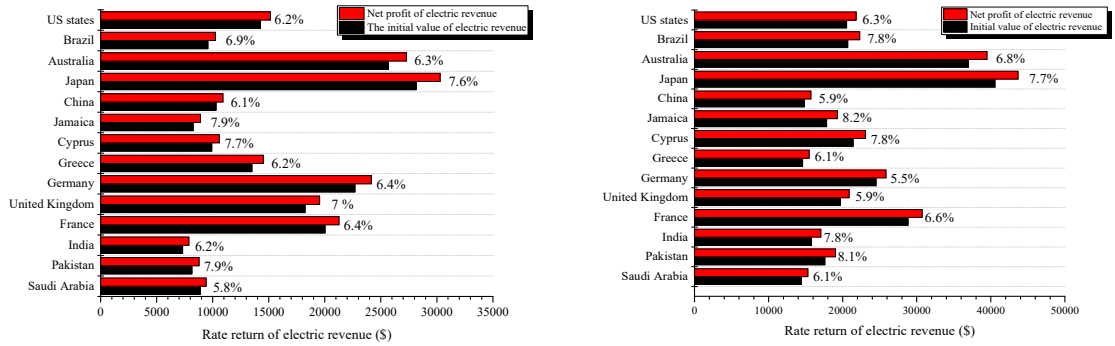

Figure 14. The increase in rate returns of electric revenue associated with the 18-kW and 43-kW 10 × 10 PV arrays, taking into account the greatest economic advantage per year.

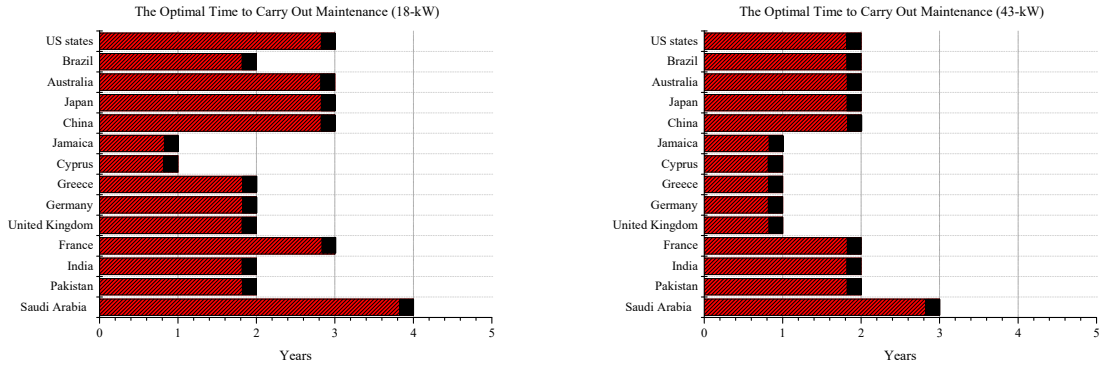

Figure 15. The year identified by the suggested algorithm as the optimal time to carry out maintenance in order to achieve the greatest economic advantage.

6. Analysis Outcomes

To establish the extent to which electric revenue can be increased to enhance economic advantages in the 14 countries analyzed, the outcomes of maintenance cost analysis for the two types of PV arrays are discussed in the following part. According to those outcomes, the suggested algorithm is arbitrarily applicable to PV arrays of different dimensions and enhanced the maximum power output for both types of PV arrays considered. Furthermore, in the first case, the algorithm considered relevant aging factors to reorganize the positions of individual PV modules in every string, thus attenuating the effect of the bypass diodes. Consequently, PV modules in all strings were less affected by mismatch losses, although voltage limits were overlooked. Other studies addressing this issue are available [7,30,35–37]. The suggested algorithm hierarchically and iteratively sorts PV modules. The generated P–V curves in Figures 10 and 13 reflect the usefulness of the strategy of PV array reconfiguration for making systems more efficient and reducing their operating costs.

Furthermore, the suggested algorithm can yield results speedily because it does not need access to all potential online and offline configurations for a given PV array, thus simplifying the process. For instance, the algorithm determined the best PV module configuration in the first case based on just nine steps, with an average computational time of 0.129375 s. Thus, by identifying the ideal module configuration rapidly, the algorithm accelerates the real-time implementation process. The suggested algorithm is also advantageous because it involves reorganization solely of the affected PV modules, leaving the others unchanged. Moreover, in the first case, the reorganization enhanced the efficiency of maintenance management. Costs and advantages are the main determinants of offline reconfiguration methods. Such methods are needed to make reconfiguration more efficient, more profitable, and more cost-effective in terms of labor since the creation of an aging map

for PV plants is essential. Reconfiguration as a way of capitalizing on the strengths of a PV plant is justified when the profitability engendered by higher power production offsets the costs of labor force reorganization. Taking these aspects into account, the suggested approach is useful as it involves the substitution of only PV module positions based on manpower rather than complete substitution of aging modules with new ones.

An overview of the approach that has been put forth in the present study in order to address the intended research question is provided in the following part. More specifically, two particular strategies were identified as a viable way to make solar power plants more efficient, on the one hand, and to achieve higher financial returns, on the other hand, on the basis of the application of a suitable reconfiguration. The proposed strategies were underpinned by the GEA, which is an algorithm that is capable of both simulation and analysis of the potential manner in which aging PV arrays can be reorganized as well as of the output power and economic advantages associated with the various solutions of reorganization. Hence, the first case study revealed that the reorganization of the PV modules that showed signs of aging acceptably improved the output power of the PV array and at the same time, increased the electric revenue. Meanwhile, the second case study also demonstrated a rise in the output power of the PV array as well as a marked increase in financial returns; this was attributed to the fact that the suggested algorithm helped to establish the best reconfiguration not only in terms of identifying the PV modules that had to be position swapped, but also in terms of identifying the PV modules that had to be substituted completely. The following example can serve to illustrate the capability of the suggested algorithm. Based on the instruction given by the algorithm, aged PV modules with a production of less than 0.5 p.u. should be substituted, whereas PV modules with a production higher than 0.6 p.u. should be retained; in this way, it is possible to preserve the PV modules that display signs of aging instead of recycling them. This kind of strategy can be a viable option for PV plants of a medium-to-large size that require maintenance. The extent to which the application of the suggested algorithm can increase the financial returns of electric revenue is indicated in Table 14, with the figures being expressed as a percentage.

Table 14. Comparative analysis of electric revenue rate returns in 14 countries over a period of one decade.

	Case One (Swapping Age Modules)				**Case Two (Swap/Replace Age Modules)**			
Country	**Net Profit of Electric Revenue 18-kW ($)**	**Profits Return**	**Net Profit of Electric Revenue 43-kW ($)**	**Profits Return**	**Net Profit of Electric Revenue 18-kW ($)**	**Profits Return**	**Net Profit of Electric Revenue 43-kW ($)**	**Profits Return**
Saudi Arabia	18,484.95	2.39%	33,953.36	0.97%	9416.8	5.8%	15,295.37	6.1%
Pakistan	4229.61	2.72%	8900.85	1.22%	8783.76	7.9%	19,020.1	8.1%
India	3798.81	2.8%	7997.1	1.26%	7867.36	7.6%	17,042.78	7.8%
France	48,523.01	2.12%	101,829.4	0.94%	21,269.97	6.4%	30,730.07	6.6%
United Kingdom	37,909.82	2.32%	79,630.39	1.04%	19,538.34	7.01%	20,868.43	5.9%
Germany	58,940.38	2.25%	123,766.96	1.01%	24,155.06	6.4%	25,853.31	5.5%
Greece	21,030.55	2.52%	44,216.77	1.13%	14,529.37	7.6%	15,466.33	6.1%
Cyprus	20,599.76	2.69%	43,344.03	1.21%	10,577.76	7.7%	23,080.62	7.8%
Jamaica	8576.71	3.38%	18,103.05	1.53%	8915.38	7.9%	19,296.4	8.2%
China	17,819.18	2.03%	44,919.83	1.05%	10,920.11	6.1%	15,696.32	5.9%
Japan	48,757.98	2.02%	122,907.76	1.04%	30,292.47	7.6%	43,673.97	7.7%
Australia	62,230.07	2.04%	149,353.52	1.01%	27,300.42	6.3%	39,483.71	6.8%
Brazil	14,921.12	2.48%	31,365.88	1.11%	10,233.3	6.9%	22,302.15	7.8%
US states	29,607.26	2.08%	72,562.45	1.05%	151,42.56	6.2%	21,825.01	6.3%

7. Conclusions

A persistent issue for PV arrays of large scale is that PV modules do not age homogeneously. If this is not addressed, this issue diminishes the PV array output power and causes PV module deterioration. Standard online global-MPPT methods are limited in monitoring the affected maximum instead of the maximum possible power of PV arrays with heterogeneous aging, with no attempt to reorganize such PV arrays. Therefore, a new algorithm for 10 × 10 PV array reconfiguration was put forth in this study, considering the costs associated with labor force and electric power in fourteen countries, namely, Saudi Arabia, Pakistan, India, France, the UK, Germany, Greece, Cyprus, Jamaica, China, Japan, Australia, Brazil, and the U.S. Due to cost discrepancies between the examined countries, the outcomes obtained were more favorable in both case studies related to the reconfiguration of aged PV modules and the substitution of aged PV modules with new ones (Tables 8 and 13), where switching the positions of the PV panels led to a slight increase in the output power of the PV array.

Nevertheless, the advantage gained in terms of electric revenue enhanced production and decreased maintenance costs over the period of a decade in the investigated countries. Hence, the approach applied in the first case and second case could also be employed for the maintenance of aged PV arrays in other countries (e.g., South Africa, Turkey, etc.). It can be concluded that based on the suggested algorithm, solar power plants can achieve better financial increment within a decade.

Author Contributions: Conceptualization, M.A.; Methodology, M.A.; Software, M.A. and Y.H.; Validation, C.S.K. and A.M.; Formal analysis, M.A. and C.S.K.; Investigation, M.A. and A.M.; Resources, M.A.; Data curation, M.A.; Writing—Original draft preparation, M.A.; Writing—Review and editing, Y.H. and C.S.K.; Visualization, M.H.A. and A.M.; Supervision, Y.H.; Project administration, Y.H., M.A.A., M.H.A., and K.E. All authors have read and agreed to the published version of the manuscript.

Funding: This research was funded by [Scientific Research Deanship at the University of Ha'il–Saudi Arabia] project number [RG-20 121].

Institutional Review Board Statement: Not applicable.

Informed Consent Statement: Not applicable.

Data Availability Statement: Data sharing not applicable.

Acknowledgments: This research was funded by the Scientific Research Deanship at the University of Ha'il–Saudi Arabia, through project number RG-20 121.

Conflicts of Interest: The authors declare no conflict of interest.

References

1. Dida, M.; Boughali, S.; Bechki, D.; Bouguettaia, H. Output power loss of crystalline silicon photovoltaic modules due to dust accumulation in Saharan environment. *Renew. Sustain. Energy Rev.* **2020**, *124*, 109787. [CrossRef]
2. Hu, Y.; Zhang, J.; Wu, J.; Cao, W.; Tian, G.Y.; Kirtley, J.L. Efficiency Improvement of Nonuniformly Aged PV Arrays. *IEEE Trans. Power Electron.* **2017**, *32*, 1124–1137. [CrossRef]
3. Alkahtani, M.; Hu, Y.; Wu, Z.; Kuka, C.S.; Alhammad, M.S.; Zhang, C. Gene Evaluation Algorithm for Reconfiguration of Medium and Large Size Photovoltaic Arrays Exhibiting Non-Uniform Aging. *Energies* **2020**, *13*, 1921. [CrossRef]
4. Osterwald, C.R.; Anderberg, A.; Rummel, S.; Ottoson, L. Degradation analysis of weathered crystalline-silicon PV modules. In Proceedings of the Conference Record of the Twenty-Ninth IEEE Photovoltaic Specialists Conference, New Orleans, LA, USA, 19–24 May 2002; pp. 1392–1395.
5. Ndiaye, A.; Kébé, C.M.F.; Ndiaye, P.A.; Charki, A.; Kobi, A.; Sambou, V. A Novel Method for Investigating Photovoltaic Module Degradation. *Energy Procedia* **2013**, *36*, 1222–1231. [CrossRef]
6. Munoz, M.A.; Alonso-García, M.C.; Vela, N.; Chenlo, F. Early degradation of silicon PV modules and guaranty conditions. *Solar Energy* **2011**, *85*, 2264–2274. [CrossRef]
7. Hu, Y.; Zhang, J.; Li, P.; Yu, D.; Jiang, L. Non-Uniform Aged Modules Reconfiguration for Large-Scale PV Array. *IEEE Trans. Device Mater. Reliab.* **2017**, *17*, 560–569. [CrossRef]

8. Orozco-Gutierrez, M.L.; Spagnuolo, G.; Ramirez-Scarpetta, J.M.; Petrone, G.; Ramos-Paja, C.A. Optimized Configuration of Mismatched Photovoltaic Arrays. *IEEE J. Photovol.* **2016**, *6*, 1210–1220. [CrossRef]
9. Velasco-Quesada, G.; Guinjoan-Gispert, F.; Pique-Lopez, R.; Roman-Lumbreras, M.; Conesa-Roca, A. Electrical PV Array Reconfiguration Strategy for Energy Extraction Improvement in Grid-Connected PV Systems. *IEEE Trans. Ind. Electron.* **2009**, *56*, 4319–4331. [CrossRef]
10. Tanesab, J.; Parlevliet, D.; Whale, J.; Urmee, T. Dust Effect and its Economic Analysis on PV Modules Deployed in a Temperate Climate Zone. *Energy Procedia* **2016**, *100*, 65–68. [CrossRef]
11. Alahmad, M.; Chaaban, M.A.; Lau, S.k.; Shi, J.; Neal, J. An adaptive utility interactive photovoltaic system based on a flexible switch matrix to optimize performance in real-time. *Solar Energy* **2012**, *86*, 951–963. [CrossRef]
12. Schultz-Wittmann, O.; Glunz, S.; Willeke, G. Multicrystalline Silicon Solar Cells Exceeding 20% Efficiency. *Prog. Photovol. Res. Appl.* **2004**, *12*, 553–558. [CrossRef]
13. Zhang, H.; Lu, Y.; Han, W.; Zhu, J.; Zhang, Y.; Huang, W. Solar energy conversion and utilization: Towards the emerging photo-electrochemical devices based on perovskite photovoltaics. *Chem. Eng. J.* **2020**, *393*, 124766. [CrossRef]
14. Li, W.; Li, W.; Xiang, X.; Hu, Y.; He, X. High Step-Up Interleaved Converter With Built-In Transformer Voltage Multiplier Cells for Sustainable Energy Applications. *IEEE Trans. Power Electr.* **2014**, *29*, 2829–2836. [CrossRef]
15. Hu, Y.; Deng, Y.; Liu, Q.; He, X. Asymmetry Three-Level Gird-Connected Current Hysteresis Control With Varying Bus Voltage and Virtual Oversample Method. *IEEE Trans. Power Electr.* **2014**, *29*, 3214–3222. [CrossRef]
16. Rabaia, M.K.H.; Abdelkareem, M.A.; Sayed, E.T.; Elsaid, K.; Chae, K.-J.; Wilberforce, T.; Olabi, A.G. Environmental impacts of solar energy systems: A review. *Sci. Total Environ.* **2021**, *754*, 141989. [CrossRef] [PubMed]
17. Alkahtani, M.; Wu, Z.; Kuka, C.S.; Alahammad, M.S.; Ni, K. A Novel PV Array Reconfiguration Algorithm Approach to Optimising Power Generation across Non-uniformly Aged PV Arrays by merely Repositioning. *J. Multidisc. Sci. J.* **2020**, *3*, 32–53. [CrossRef]
18. Soliman, M.A.; Hasanien, H.M.; Alkuhayli, A. Marine Predators Algorithm for Parameters Identification of Triple-Diode Photovoltaic Models. *IEEE Access* **2020**, *8*, 155832–155842. [CrossRef]
19. Takashima, T.; Yamaguchi, J.; Otani, K.; Oozeki, T.; Kato, K.; Ishida, M. Experimental studies of fault location in PV module strings. *Solar Energy Mater. Solar Cells* **2009**, *93*, 1079–1082. [CrossRef]
20. Meyer, E.L.; Dyk, E.E.v. Assessing the reliability and degradation of photovoltaic module performance parameters. *IEEE Trans. Reliab.* **2004**, *53*, 83–92. [CrossRef]
21. Hu, Y.; Cao, W.; Wu, J.; Ji, B.; Holliday, D. Thermography-Based Virtual MPPT Scheme for Improving PV Energy Efficiency Under Partial Shading Conditions. *IEEE Trans. Power Electr.* **2014**, *29*, 5667–5672. [CrossRef]
22. Kumar, R.A.; Suresh, M.S.; Nagaraju, J. Measurement of AC parameters of gallium arsenide (GaAs/Ge) solar cell by impedance spectroscopy. *IEEE Trans. Electron Dev.* **2001**, *48*, 2177–2179. [CrossRef]
23. Mattei, M.; Notton, G.; Cristofari, C.; Muselli, M.; Poggi, P. Calculation of the polycrystalline PV module temperature using a simple method of energy balance. *Renew. Energy* **2006**, *31*, 553–567. [CrossRef]
24. Chouder, A.; Silvestre, S. Automatic supervision and fault detection of PV systems based on power losses analysis. *Energy Convers. Manag.* **2010**, *51*, 1929–1937. [CrossRef]
25. Silvestre, S.; Chouder, A.; Karatepe, E. Automatic fault detection in grid connected PV systems. *Solar Energy* **2013**, *94*, 119–127. [CrossRef]
26. Nguyen, D.; Lehman, B. An Adaptive Solar Photovoltaic Array Using Model-Based Reconfiguration Algorithm. *IEEE Trans. Ind. Electron.* **2008**, *55*, 2644–2654. [CrossRef]
27. Storey, J.P.; Wilson, P.R.; Bagnall, D. Improved Optimization Strategy for Irradiance Equalization in Dynamic Photovoltaic Arrays. *IEEE Trans. Power Electr.* **2013**, *28*, 2946–2956. [CrossRef]
28. Storey, J.; Wilson, P.R.; Bagnall, D. The Optimized-String Dynamic Photovoltaic Array. *IEEE Trans. Power Electr.* **2014**, *29*, 1768–1776. [CrossRef]
29. Cristaldi, L.; Faifer, M.; Rossi, M.; Toscani, S.; Catelani, M.; Ciani, L.; Lazzaroni, M. Simplified method for evaluating the effects of dust and aging on photovoltaic panels. *Measurement* **2014**, *54*, 207–214. [CrossRef]
30. Wu, Z.; Zhang, C.; Alkahtani, M.; Hu, Y.; Zhang, J. Cost Effective Offline Reconfiguration for Large-Scale Non-Uniformly Aging Photovoltaic Arrays Efficiency Enhancement. *IEEE Access* **2020**, *8*, 80572–80581. [CrossRef]
31. Global Petrp Prices. Electricity Prices around the World. Available online: https://www.globalpetrolprices.com/electricity_prices/ (accessed on 20 November 2020).
32. Salary Expert. Electrician Salary. Available online: https://www.salaryexpert.com/salary/job/electrician/ (accessed on 25 November 2020).
33. Lazard. Levelized Cost of Energy and Levelized Cost of Storage–2020. Available online: https://www.lazard.com/perspective/levelized-cost-of-energy-and-levelized-cost-of-storage-2020/ (accessed on 25 November 2020).
34. IRENA. Renewable Power Generation Costs-2019. Available online: https://www.irena.org/publications/2020/Jun/Renewable-Power-Costs-in-2019 (accessed on 25 November 2020).
35. Djordjevic, S.; Parlevliet, D.; Jennings, P. Detectable faults on recently installed solar modules in Western Australia. *Renew. Energy* **2014**, *67*, 215–221. [CrossRef]

36. Wang, Z.; Zhou, N.; Gong, L.; Jiang, M. Quantitative estimation of mismatch losses in photovoltaic arrays under partial shading conditions. *Optik* **2020**, *203*, 163950. [CrossRef]
37. Nobile, G.; Vasta, E.; Cacciato, M.; Scarcella, G.; Scelba, G.; Stefano, A.G.F.D.; Leotta, G.; Pugliatti, P.M.; Bizzarri, F. Study on mismatch losses in large PV plants: Data analysis of a case study and modeling approach. In Proceedings of the 2020 International Symposium on Power Electronics, Electrical Drives, Automation and Motion (SPEEDAM), Sorrento, Italy, 24–26 June 2020; pp. 858–864.